Sulfate Adsorption on a Volcanic Ash Soil (Allophanic Andisol) under Low pH Conditions

Munehide Ishiguro*[,1], Tomoyuki Makino[2]

[1] *Graduate School of Environmental Science, Okayama University, 3-1-1. Tsushima-naka, Kitaku, Okayama 700-8530, Japan*

[2] *Soil Environment Division, National Institute for Agro-Environmental Sciences, 3-1-3 Kannondai, Tsukuba, 305-8604, Japan*

* Corresponding author

Tel./fax: +81 86 251 8875

E-mail adress: ishi@cc.okayama-u.ac.jp (M. Ishiguro)

ABSTRACT

The mechanisms of SO_4 adsorption on clays have been investigated by many researchers. However, few researches have focused on the fraction of SO_4 that is adsorbed in the diffuse layer to the total adsorbed SO_4. We investigated SO_4 adsorption in detail on an allophanic Andisol (volcanic ash soil), especially the fraction of SO_4 adsorbed in the diffuse layer to the total adsorbed SO_4, conducting experiments under conditions of low pH (pH 3.3 and 4.3) and low ion concentrations (1.0 and 0.1 $mol_c\ m^{-3}$) to avoid a strong negative surface charge of the soil particles. SO_4 and NO_3 adsorption under their competitive conditions were measured by a batch method using mixtures of HNO_3 and H_2SO_4. Exchangeable SO_4 and NO_3 were extracted with 1000 $mol_c\ m^{-3}$ KCl. Strongly adsorbed SO_4 was extracted with 10 $mol_c\ m^{-3}$ NaOH after the extraction with 1000 $mol_c\ m^{-3}$ KCl. The exchangeable SO_4 made up 72 to 77 % of the total adsorbed SO_4. These results suggested that both inner-sphere and outer-sphere complexes co-exist in the allophanic Andisol at low pH. SO_4 was strongly selective over NO_3 under these conditions. We compared adsorbed amounts calculated by the Gouy-Chapman model with the measured values at solution conditions of pH 3.3 and 1.0 $mol_c\ m^{-3}$. The model overestimated NO_3 adsorption and underestimated SO_4 adsorption. The difference is due to the fact that SO_4 adsorption in the Stern layer is neglected. Next, we calculated SO_4 adsorbed in the diffuse layer using the Stern-Gouy-Chapman model under the assumption that all the measured NO_3 adsorbed was in the diffuse layer. Our results indicated that the SO_4 in the diffuse layer made up only less than 6 % of the total adsorbed SO_4. Most of the adsorbed SO_4 is likely to be found in direct contact with the soil surface.

Key Words: allophanic Andisol, volcanic ash soil, nitrate adsorption,

Stern-Gouy-Chapman model, sulfate adsorption, surface complexation

1. Introduction

The position of the adsorbed counterions on clays affects the soil structure. When the counterions are adsorbed only directly on the clay surface, the clay surface potential becomes small and the clay flocculates. On the other hand, when the counterions are adsorbed in the diffuse layers and thick diffuse layers develop, the clay swells or disperses due to the repulsive force of overlapping diffuse layers.

Allophanic Andisol (volcanic ash soil) contains a substantial amount of pH-dependent charges. The positive charge becomes predominant at low pH and the negative charge becomes predominant at high pH [1-4]. Thus, the soil disperses at low and high pH [3]. However, the soil suspension flocculates in dilute H_2SO_4 solution, while it disperses in dilute HNO_3 solution [5,6]. Ishiguro and Nakajima [6] suggested that weaker repulsive forces compared to attractive forces among soil particles cause flocculation in dilute H_2SO_4 solution because SO_4 is divalent and is strongly adsorbed on soils with pH-dependent charges. Ishiguro et al. [7] showed that repulsive potential energy between the soil clays decreased when SO_4 was adsorbed.

SO_4 is strongly adsorbed on allophanic clays and soils [8,9]. It induces NO_3 leaching due to its strong adsorption [10]. However, the mechanism of SO_4 adsorption at the clay-water interface has been a source of debate. Many researchers have indicated that SO_4 forms an inner-sphere surface complex on hydrous alumina [11], allophanic clays [9], kaolinitic Alfisols [12], hematite [13], and amorphous iron hydroxide [14]. On the other hand, other researchers showed that SO_4 does not form chemical coordination on the surface, or the sorption can largely be explained by electrostatic considerations [15-20]. Spectroscopic results [21-23] suggest that SO_4 forms both outer-sphere and inner-sphere surface complexes on goethite, and the ratio of the latter complex increases

with decreasing pH. SO_4 adsorption on goethite was evaluated with the Charge Distribution Multisite Complexation model and compared with the spectroscopic analysis [24]. Ishiguro et al. [25] indicated SO_4 surface precipitation, stronger and weaker SO_4 adsorption sites on allophanic soil by using theoretical adsorption isotherms. Prietzel et al. [26] showed that adsorbed SO_4 can be distinguished from SO_4 precipitated in soils by X-ray Absorption Near Edge Structure (XANES).

However, the SO_4 proportion of that adsorbed in direct contact with the soil surface to that in the diffuse layer has not been discussed in the studies. Therefore, in the present study, we evaluated the amount of SO_4 in the diffuse layer and the Stern layer for an allophanic Andisol under low pH and low concentration conditions. Low pH and low concentration conditions were selected because the positive charge was predominant and the negative charge could be neglected. SO_4 and NO_3 adsorption under their respective competitive conditions were measured by a batch method. Results were compared to predictions based on the Gouy-Chapman model. SO_4 adsorbed in the diffuse layer and the Stern layer were evaluated with the Stern-Gouy-Chapman model.

2. Materials and Methods

2.1. Soil

Allophanic Andisol was obtained from a field at the National Institute for Agro-Environmental Sciences in Tsukuba, Japan, from the 4Bw1 horizon of Typic Dystrandep [27]. Its physical and chemical properties measured by the National Institute of Agricultural Sciences [28] are listed in Table 1. The specific surface of

the soil obtained from N_2 adsorption was 211 m^2 g^{-1} (QUANTACHROME AUTOSORB-1). Fresh raw soil sample, which had been passed through 2-mm-mesh sieves, was used in the experiment.

2.2. Anion Adsorption Experiments

NO_3 and SO_4 adsorptions, as well as the anion exchange capacity (AEC), were measured using the batch method of Wada and Okamura [29] with minor modification. AEC is defined herein as the sum of exchangeable anions extracted with 1000 mol_c m^{-3} KCl solution. A NaOH solution at 10 mol_c m^{-3} was used as an extraction solution for strongly adsorbed SO_4, which was not extracted with a 1000 mol_c m^{-3} KCl solution.

Solutions used for the equilibration according to step 1, mentioned below, were six different mixtures of $NaNO_3$ and Na_2SO_4 at a total electrolyte concentration of 1000 mol_c m^{-3}. Solutions used for the final equilibration according to step 2 were six different mixtures of HNO_3 and H_2SO_4 at pH 3 or pH 4. The mixed solutions at pH 3 and pH 4 were equivalent to total electrolyte concentrations of 1.0 and 0.1 mol_c m^{-3}, respectively. Mixed ratios of SO_4 concentration (mol_c m^{-3}) to NO_3+SO_4 concentration (mol_c m^{-3}) in those solutions (SO_4 ratio) were 0, 13, 30, 50, 75, and 100 %. The procedure was as follows:

Step 1 (equilibration with electrolytes at 1000 mol_c m^{-3}). Approximately 2 g of soil sample was equilibrated overnight with 200 cm^3 of the mixture of $NaNO_3$ and Na_2SO_4 at 1000 mol_c m^{-3} and a specified SO_4 ratio. The soil solution pH was roughly adjusted to pH 3 or 4 with HNO_3 or H_2SO_4. The soil sample was centrifuged for 10 min at 3 000 rpm (1 900 g), and the supernatant was discarded.

Step 2 (final equilibration with electrolytes at 0.1 or 1.0 mol_c m^{-3}). The soil sample

roughly adjusted to pH 3 was shaken for 1 h with 200 cm^3 of the mixture of HNO_3 and H_2SO_4 at 1.0 mol_c m^{-3} and a specified SO_4 ratio. The soil sample roughly adjusted to pH 4 was shaken with the mixture of HNO_3 and H_2SO_4 at 0.1 mol_c m^{-3} and a specified SO_4 ratio. The soil sample was then centrifuged for 30 min at 12 000 rpm (15 000 g), and the supernatant was discarded. This procedure was repeated six times. The final supernatant was filtrated through a disposable membrane filter, pore size 0.2 μm, with a 10-mL disposable plastic syringe and kept to analyze the concentrations of SO_4, NO_3, H and Al. The final pH of the supernatant became pH 3.3±0.1 for 1.0 mol_c m^{-3} solution and pH 4.3±0.1 for 0.1 mol_c m^{-3} solution.

Step 3 (extraction with KCl). The centrifuged and decantated soil sample was shaken with 60 cm^3 of 1000 mol_c m^{-3} KCl for 15 min. The soil sample was then centrifuged for 10 min at 3000 rpm (1900 g), and the supernatant was collected. This procedure was repeated three times. The collected supernatant was filtrated as mentioned at step 2 and kept to analyze the concentrations of SO_4, NO_3 and H.

Step 4 (extraction with NaOH). The soil sample obtained after extraction with KCl was shaken with 200 cm^3 of 10 mol_c m^{-3} NaOH for 15 min. The mixture was then centrifuged, and the supernatant was collected. This procedure was repeated twice. The collected supernatant was filtrated as mentioned at step 2 and kept to analyze the SO_4 concentration.

The NO_3 concentrations of the supernatants were measured by the steam distillation method [30], and the SO_4 concentrations were measured by ion chromatography (IC-500S, Yokogawa Electric Corporation). The NO_3 and SO_4 adsorbed amounts were then calculated from the difference with the amounts in the original solutions remained in the soils after decantation at step 2. A reliable NO_3 adsorbed amount could not be

derived under pH 4.3 condition except for 100 % NO_3 ratio (=0 % SO_4 ratio), because concentrations in the collected solution with the KCl extraction were too low. The H concentrations of the supernatant were measured with a pH meter. The Al concentrations of the supernatant were measured by Inductively Coupled Plasma - Optical Emission Spectrometry (ICP-OES) (MaximIII, Applied Research Laboratories).

2.3. Application of the Gouy-Chapman Model

To simplify the model calculation, the soil clay surface is assumed to be a flat plane. The charge density of the clay was calculated from the measured AEC, the clay content, and specific surface of the soil. If all exchangeable ions are present in the diffuse layer, the Gouy-Chapman model (GC model) can be applied. In this case, the relationship between the surface potential of the clay, Ψ_s, and its surface charge density, σ, is derived from the Poisson-Boltzmann equation [31]:

$$\begin{aligned}\sigma^2 = {} & 2\varepsilon RT[NO_3]\left\{\exp\left(\frac{F\Psi_S}{RT}\right)-1\right\}+2\varepsilon RT[SO_4]\left\{\exp\left(\frac{2F\Psi_S}{RT}\right)-1\right\} \\ & +2\varepsilon RT[H]\left\{\exp\left(-\frac{F\Psi_S}{RT}\right)-1\right\}+2\varepsilon RT[Al]\left\{\exp\left(-\frac{3F\Psi_S}{RT}\right)-1\right\}\end{aligned} \quad (1)$$

where, [ ] is ion concentration in the bulk solution, ε is the permittivity of the water, R is the gas constant, T is the absolute temperature, and F is the Faraday constant. Ψ_s is calculated from Eq. (1) when the charge density is given.

The potential distribution in the diffuse layer is given by the following approximation derived from the Poisson-Boltzmann equation:

$$\left(\frac{d\Psi}{dx}\right)^2 = \frac{2RT}{\varepsilon}[NO_3]\left\{\exp\left(\frac{F\Psi}{RT}\right)-1\right\}+\frac{2RT}{\varepsilon}[SO_4]\left\{\exp\left(\frac{2F\Psi}{RT}\right)-1\right\} + \frac{2RT}{\varepsilon}[H]\left\{\exp\left(-\frac{F\Psi}{RT}\right)-1\right\}+\frac{2RT}{\varepsilon}[Al]\left\{\exp\left(-\frac{3F\Psi}{RT}\right)-1\right\} \quad (2)$$

where x is the distance from the clay surface and Ψ is the potential at x [30]. The potential at x+Δx, Ψ(x+Δx), is calculated by the explicit finite difference method as follows;

$$\Psi(x+\Delta x) = \left[\frac{2RT}{\varepsilon}[NO_3]\left\{\exp\left(\frac{F\Psi(x)}{RT}\right)-1\right\}+\frac{2RT}{\varepsilon}[SO_4]\left\{\exp\left(\frac{2F\Psi(x)}{RT}\right)-1\right\} + \frac{2RT}{\varepsilon}[H]\left\{\exp\left(-\frac{F\Psi(x)}{RT}\right)-1\right\}+\frac{2RT}{\varepsilon}[Al]\left\{\exp\left(\frac{3F\Psi(x)}{RT}\right)-1\right\}\right]^{\frac{1}{2}}\Delta x + \Psi(x) \quad . (3)$$

where Δx is the increment of distance and Ψ(x) is the potential at x, which is derived by iteration with Eq.(3) from Ψ_s at the clay surface.

Next, we obtain the anion concentration distribution in the diffuse layer as follows:

$$C_i(x) = C_{0,i}\exp\left(-\frac{z_i F\Psi}{RT}\right) \quad (4)$$

where $C_i(x)$ is the concentration of anion i at x, $C_{0,i}$ is the bulk concentration of anion i, and z_i is the valence of anion i. We then obtain the approximated adsorbed amount of the anion i for the GC model, $q_{G,i}$.

$$q_{G,i} = \int_0^d \{C_i(x) - C_{0,i}\}dx \quad (5)$$

where d is the distance over which the potential in the diffuse layer vanishes; we put $d=20\kappa^{-1}$, where κ^{-1} is the Debye length which is often called the "thickness" of the diffuse layer.

In this model, the amounts of NO_3 and SO_4 adsorbed in the diffuse layer are

calculated using the measured values; the AEC, the clay content, the specific surface of the soil, and the equilibrium bulk concentrations of NO_3, SO_4, H and Al. No fitting parameters are required.

2.4. Application of the Stern-Gouy-Chapman model

If some of the exchangeable SO_4 is adsorbed in the Stern layer, the Stern-Gouy-Chapman model (SGC model) must be used instead of the GC model. Because NO_3 is an indifferent ion and the NO_3 concentrations in the experiment were dilute (< 1.0 mol_c m^{-3}), we assumed that all the adsorbed NO_3 exists in the diffuse layer. Having measured the total adsorbed amounts of NO_3 and SO_4, we can estimate the amounts of SO_4 adsorbed in the Stern layer and those in the diffuse layer by using the SGC model. Because the potential distribution in the diffuse layer is determined by the bulk solution conditions as shown in Eq. (2), the concentration distributions derived in the GC model can also be used in this case.

The measured amount of adsorbed NO_3 per unit surface area, $Q(NO_3)$, is equal to the diffuse NO_3 adsorption:

$$Q(\mathrm{NO_3}) = \int_a^d \left\{C_{NO_3}(x) - C_{0,NO_3}\right\} dx \qquad (6)$$

where a is the location of the Stern plane in the SGC model, that is, the distance of the diffuse layer in this model is $d - a$, as the value of d and the potential distribution calculated from the GC model are used. The a value is derived with Eq.(6); $Q(NO_3)$ is the measured value, $C_{NO3}(x)$ is already obtained as the result of the GC model with Eq.(4) and $C_{0,NO3}$ is the known equilibrium concentration, then, the a value can be obtained. We can then calculate the amount of adsorbed SO_4 in the diffuse layer,

$q_D(SO_4)$.

$$q_D(SO_4) = \int_a^d \{C_{SO_4}(x) - C_{0,SO_4}\} dx \quad (7)$$

The amount of SO_4 adsorbed in the Stern layer, $q_S(SO_4)$, is

$$q_S(SO_4) = Q(SO_4) - q_D(SO_4) \quad (8)$$

where $Q(SO_4)$ is the measured amount of adsorbed SO_4 per unit surface area.

In this model, SO_4 adsorbed amount in the diffuse layer is calculated using the measured values, listed earlier in the GC model section, plus the NO_3 adsorbed amount. The equilibrium bulk concentrations of NO_3, SO_4, H and Al are also used for the calculation of Ψ in Eq. (3). No fitting parameters are required.

3. Results

The experimental results of the anion adsorptions are shown in Figs. 1 and 2. The results at pH 3.3 and 1.0 $mol_c\ m^{-3}$ are given in Fig. 1. The NO_3 adsorption was measured by extraction with 1000 $mol_c\ m^{-3}$ KCl. The AEC is the sum of the NO_3 adsorption and the exchangeable SO_4 adsorption measured by extraction with 1000 $mol_c\ m^{-3}$ KCl. The total anion adsorption is the sum of the AEC and the strong SO_4 adsorption measured by extraction with 10 $mol_c\ m^{-3}$ NaOH. The amount of exchangeable SO_4 measured by extraction with 1000 $mol_c\ m^{-3}$ KCl, is the difference between the AEC and the NO_3 adsorption in Fig. 1. These values ranged from 72 % to 74 % of the total anion adsorption at SO_4 ratios between 13 % and 100 %. The amount of strongly adsorbed SO_4, which was measured by extraction with 10 $mol_c\ m^{-3}$ NaOH, is the difference between the total anion adsorption and the AEC. Strongly adsorbed SO_4 ranged from

26 % to 28 % of the total anion adsorption at SO_4 ratios between 13 % and 100 %. Adsorbed NO_3 was completely exchanged with 1000 $mol_c\ m^{-3}$ KCl. The NO_3 adsorption at 0 % SO_4 was 103 $mmol_c\ kg^{-1}$, while the exchangeable SO_4 adsorption at 100 % SO_4 was 294 $mmol_c\ kg^{-1}$. NO_3 adsorption at SO_4 ratios between 13 % and 75 % ranged from 0.6 to 7.6 $mmol_c\ kg^{-1}$, which was only 0.2 % to 3.2 % of the AEC. SO_4 is strongly selective over NO_3 under our experimental conditions.

The adsorbed amounts at pH 4.3 and 0.1 $mol_c\ m^{-3}$ are shown in Fig.2. Although these results are similar to the results at pH 3.3, the total SO_4 adsorbed amounts were 64 % to 73 % of those at pH 3.3. The amount of strongly adsorbed SO_4, which is the difference between the total SO_4 adsorbed and the exchangeable SO_4, ranged from 23 % to 27 % of the total SO_4 adsorption at SO_4 ratios between 13 % and 100 % similar to the results adsorbed at pH 3.3. The NO_3 adsorbed amount for 100 % NO_3 ratio (0 % SO_4 ratio) at pH 4.3 was 33.9 $mmol_c\ kg^{-1}$, which was 32.9 % of that at pH 3.3.

We could not adapt the GC model or the SGC model to the condition at pH 4.3 due to our inability to determine the NO_3 adsorbed amount. Therefore, only the results for the pH 3.3 were calculated. Adsorbed amounts calculated by the GC model are compared with the measured values in Fig. 3. The GC model overestimated NO_3 adsorption and underestimated SO_4 adsorption.

The SGC model was applied to the results at the pH 3.3, calculating the SO_4 in the diffuse layer with the assumption that all the measured NO_3 adsorbed was in the diffuse layer. The calculated SO_4 in the diffuse layer, measured strongly adsorbed SO_4, and measured exchangeable SO_4 are shown in Fig. 4. The SO_4 in the diffuse layer made up only 1.7 % to 6.1 % of the total adsorbed SO_4. The amount of exchangeable SO_4 in the Stern layer is the difference between the exchangeable SO_4 and the SO_4 in the diffuse layer shown in Fig. 4. These values ranged from 68 % to 72 % of the total adsorbed

SO_4 at SO_4 ratios between 13 % and 75 %. The strongly adsorbed SO_4 ranged from 26 % to 28 % of the total adsorbed SO_4 at SO_4 ratios between 13 % and 100 %.

4. Discussion

The GC model neglected the exchangeable SO_4 adsorbed in the Stern layer. However, when the SGC model was adopted, about 92 % to 98 % of the exchangeable SO_4 was adsorbed in the Stern layer. This amount could not be negligible, and it clearly accounts for the disagreement between the measured and the calculated values in Fig. 3.

Under the SGC model, the sum of SO_4 adsorbed in the Stern layer and the strongly adsorbed SO_4 became 94 % to 98 % of the total adsorbed SO_4, assuming that all adsorbed NO_3 was in the diffuse layer. Gibb and Koopal [32] showed that amounts of surface complexation of NO_3 on rutile and hematite were considerable at lower pH with Koopal's one-pK SGC model [33]. If we assume that some adsorbed NO_3 forms surface complexation, the SO_4 adsorbed in direct contact with the soil surface must be more than 94 % to 98 % of the total adsorbed SO_4. We conclude that most of the adsorbed SO_4 (more than 94 %) was in direct contact with the soil surface and the amount of SO_4 in the diffuse layer was very small (less than 6 %) in our experimental condition at pH 3.3.

We consider that the exchangeable SO_4 is adsorbed by electrostatic forces, and that strongly adsorbed SO_4 extracted with NaOH reflects chemical adsorption. Another reaction that must be considered is a precipitation of basic aluminum sulfates [8]. However, when the solubility product $(Al)^4(OH)^{10}SO_4=10^{-117.3}$ proposed by Singh and Brydon [34] is applied, basaluminite should not precipitate under our experimental conditions.

Both strongly adsorbed SO_4 and exchangeable SO_4 were found in our experiment,

consistent with the results of Gebhardt and Coleman [8]. Wijnja and Schulthess [23] determined that SO_4 forms both outer-sphere and inner-sphere surface complexes on alminum oxide at pH less than 6. Ishiguro et al. [25] showed both stronger and weaker adsorption sites on allophanic Andisol by using the Langmuir isotherm. In their research, most of the SO_4 was adsorbed on the stronger site and only about 2 % was adsorbed on the weaker site at pH 4 and 0.1 $mol_c\ m^{-3}$ SO_4. It is questionable whether the exchangeable and strongly adsorbed SO_4 correspond respectively to the outer-sphere and inner-sphere complex. The adsorption of the exchangeable SO_4 extracted with 1000 $mol_c\ m^{-3}$ KCl may not be entirely to electrostatic adsorption. Agbenin [12] has noted that 1000 $mol_c\ m^{-3}$ is a very high ionic strength and that under these conditions some inner-sphere complexes might be extracted. Further investigation is needed at this point.

From the results of the SGC model, nearly all of the adsorbed SO_4 (more than 94 %) was in direct contact with the soil surface and the amount of SO_4 in the diffuse layer was very small (less than 6 %) in our experimental condition at pH 3.3 for the allophanic Andisol. Therefore, the soil should flocculate under low pH, when SO_4 is the main counterion, because the effective surface charge is very low. Ishiguro and Nakajima [6] determined that the soil flocculated in H_2SO_4 at pH3 and 4, but dispersed in HNO_3 at pH3 and 4. Ishiguro et al. [7] showed that the repulsive potential energy between the soil clays became small when SO_4 was adsorbed. Their results are consistent with our experimental results.

REFERENCES

[1] Y. Okamura, K. Wada, Electric charge characteristics of horizons of Ando (B) and red-yellow-B soils and weathered pumices, J. Sil Sci. 34 (1983) 287-295.

[2] M. Ishiguro, K. Song, K. Yuita, Ion-transport in an allophanic Andisol under the influence of variable charge, Soil Sci. Soc. Am. J. 56 (1992) 1789-1793.

[3] T. Nakagawa, M. Ishiguro, Hydraulic conductivity of an allophanic andisol as affected by solution pH, J. Environ. Qual. 23 **(**1994) 208-210.

[4] N.P. Qafoku, E. Van Ranst, A. Noble, G. Baert. Variable charge soils: Their mineralogy, chemistry and management. Adv. Agron. 84 (2004) 159-215.

[5] S. Matsukawa, H. Tomita, S. Suzuki, H. Katoh, Relation between soil dispersion, hydraulic conductivity and pH of soil water for allophanic soils during acid solution leaching, (in Japanese with English summary) Soil Phys. Conditions Plant Growth Japan 77 **(**1998) 3-9.

[6] M. Ishiguro, T. Nakajima, Hydraulic conductivity of an allophanic Andisol leached with dilute acid solutions, Soil Sci. Soc. Am. J. 64 (2000) 813-818.

[7] M. Ishiguro, K. Nakaishi, T. Nakajima, Saturated hydraulic conductivity of a volcanic ash soil affected by repulsive potential energy in a multivalent anionic system, Colloids Surf. A 230 (2003) 81-88

[8] H. Gebhardt, N.T. Coleman, Anion adsorption by allophanic tropical soils: II. Sulfate adsorption, Soil Sci. Soc. Am. Proc. 38 (1974) 259-262.

[9] S.S.S. Rajan, Adsorption and desorption of sulfate and charge relationships in allophanic clays, Soil Sci. Soc. Am. J. 43 (1979) 65-69.

[10] M. Ishiguro, Y. Manabe, S. Seo, T. Akae, Nitrate transport in volcanic ash soil of A and B horizons affected by sulfate, Soil Sci. Plant Nutr. 49 (2003) 249-254.

[11] S.S.S. Rajan, Sulfate adsorbed on hydrous alumina, ligands displaced, and changes in surface charge, Soil Sci. Soc. Am. J. 42 (1978) 39-44.

[12] J.O. Agbenin, Sulfate retention by kaolinitic alfisols from Nigerian savanna, Soil Sci. Soc. Am. J. 61 (1997) 53-57.

[13] S.J. Hug, In situ transform infrared measurements of sulfate adsorption on Hematite in aqueous solutions, J. Colloid Interface Sci. 188 (1997) 415-419.

[14] N. U. Yamaguchi, M. Okazaki, T. Hashitani, Volume changes due to SO_4, SeO_4, and H_2PO_4 adsorption on amorphous Iron(III) hydroxide in an aqueous suspension, J. Colloid Interface Sci. 209 (1999) 386-391.

[15] K.B. Marsh, R.W. Tillman, J.K. Syers, Charge relationships of sulphate sorption by soils, Soil Sci. Soc. Am. J. 51 (1987) 318-323.

[16] D. Curtin, J.K. Syers, Mechanism of sulphate adsorption by two tropical soils, J. Soil Sci. 41 (1990) 295-304.

[17] D. Curtin, J.K. Syers, Extractability and adsorption of sulphate in soils, J. Soil Sci. 41 (1990) 305-312.

[18] P.C. Zhang, D.L. Sparks, Kinetics and mechanisms of sulphate adsorption/desorption on goethite using pressure-jump relaxation, Soil Sci. Soc. Am. J. 54 (1990) 1266-1273.

[19] S. Maneepong, S. Wada, Stability of Cl, NO_3, ClO_4, and SO_4 surface complexes at synthetic goethite/aqueous electrolyte interfaces, Soil Sci. Plant Nutr. 37 (1991) 141-150.

[20] L.M. He, L.W. Zelazny, V.C. Baligar, K.D. Ritchey, D.C. Martens, Ionic strength effects on sulfate and phosphate adsorption on γ-alumina and kaolinite: Triple-layer model, Soil Sci. Soc. Am. J. 61 (1997) 784-793.

[21] D. Peak, R.G. Ford, D.L. Sparks, An in situ ATR-FTIR investigation of sulfate bonding mechanisms on goethite, J. Colloid Interface Sci. 218 (1999) 289-299

[22] J.D. Ostergren, G.E. Brown Jr, G.A. Parks, P. Persson, Inorganic ligand effects on Pb(II) sorption to goethite. II.Sulfate, J. Colloid Interface Sci. 225 (2000) 483-493.

[23] H. Wijnja, C.P. Schulthess, Vibrational spectroscopy study of selenate and sulfate

adsorption mechanisms on Fe and Al (hydr)oxide surfaces, J. Colloid Interface Sci. 229 (2000) 286-297.

[24] R.P.J.J. Rietra, T. Hiemstra, W.H. van Riemsdijk, Comparison of selenate and sulfate adsorption on goethite, J. Colloid Interface Sci. 240 (2001) 384-390.

[25] M. Ishiguro, T. Makino, Y. Hattori, Sulfate Adsorption and Surface Precipitation on a Volcanic Ash Soil (Allophanic Andisol), J. Colloid Interface Sci. 300 (2006) 504-510.

[26] J. Prietzel, J. Thieme, A. Herre, M. Salomé, D. Eichert, Differentiation between adsorbed and precipitated sulphate in soils and at micro-sites of soil aggregates by sulphur K-edge XANES, Euro. J. Soil Sci. 59 (2008) 730-743.

[27] Soil Survey Staff, *Keys to Soil Taxonomy* 8th ed. USDA, National Resources Conservation Service, Washington, D.C (0988).

[28] National Institute of Agricultural Sciences, Outline of the test of soil and the major nutrients in the field of the National Institute of Agricultural Sciences, (in Japanese) Materials of Department of Chemistry, Natl. Inst. Agric. Sci. **3** (1984) 1-32.

[29] K. Wada, Y. Okamura, Electric charge characteristics of Ando A1 and buried A1 horizon soils, J. Soil Sci. 31 (1980) 307-314.

[30] R. L. Mulvaney, Steam-distillation methods. In Methods of soil analysis. Part 3-chemical methods, 1996, p.1131-1139, Soil Science Society of America, Madison

[31] P.C. Hiementz, Principles of colloid and surface chemistry, Marcel Dekker, New York, 1986, pp. 677-735.

[32] A.W.M. Gibb, L.K. Koopal, Electrochemistry of a model for patchwise heterogeneous surfaces: The rutile-hematite system, J. Colloid and Interface Sci. 134 (1990) 122-138.

[33] L.K. Koopal, Adsorption of ions and surfactants. In Coagulation and flocculation,

Ed. B Dobiáš, 1993, p.101-207, Marcel Dekker, New York

[34] S.S. Singh, J.E. Brydon, Solubility of basic aluminum sulfates at equilibrium in solution and in the presence of montmorillonite, Soil Sci. 107 (1969) 12-16.

Figure legends

Fig. 1. Anion adsorption on the allophanic Andisol at pH 3.3 and 1.0 $mol_c\ m^{-3}$.

Fig. 2. SO_4 adsorption on the allophanic Andisol at pH 4.3 and 0.1 $mol_c\ m^{-3}$.

Fig. 3. The Gouy-Chapman model estimations of NO_3 and SO_4 adsorrption compared to the experimental data at pH 3.3.

Fig. 4 SO_4 adsorption at pH 3.3. SO_4 in the diffuse layer was calculated by the Stern-Gouy-Chapman model.

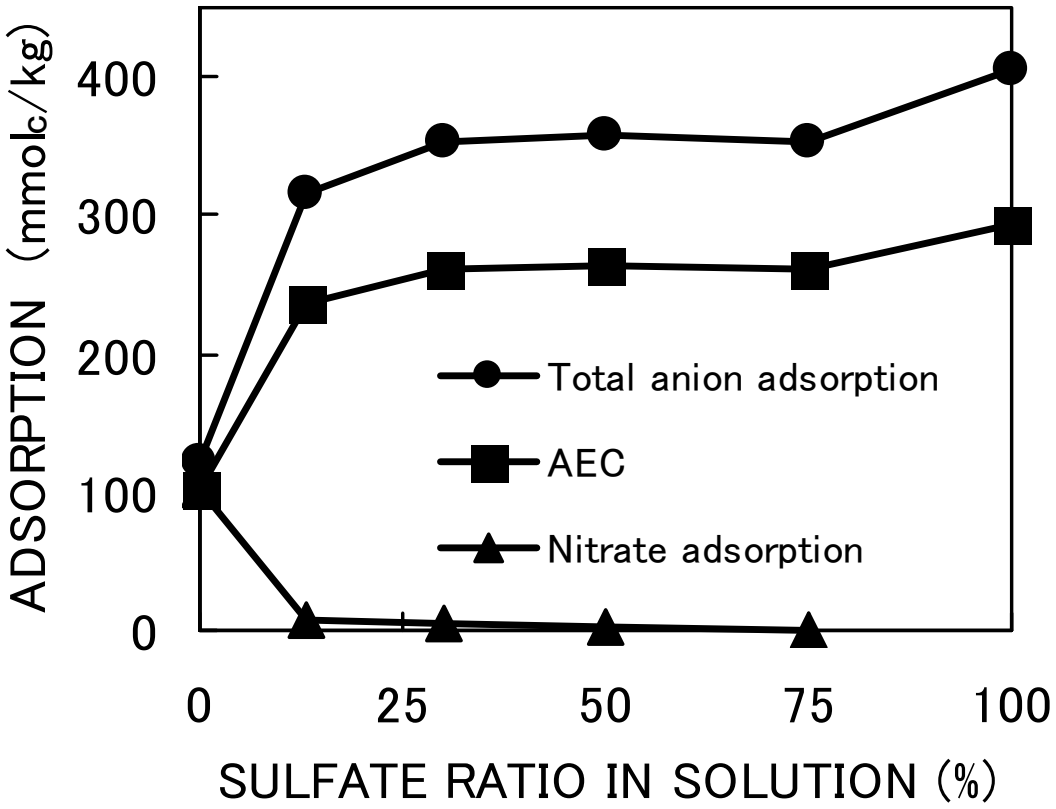

Fig. 1. Anion adsorption on the allophanic Andisol at pH 3.3 and 1.0 $mol_c\ m^{-3}$.

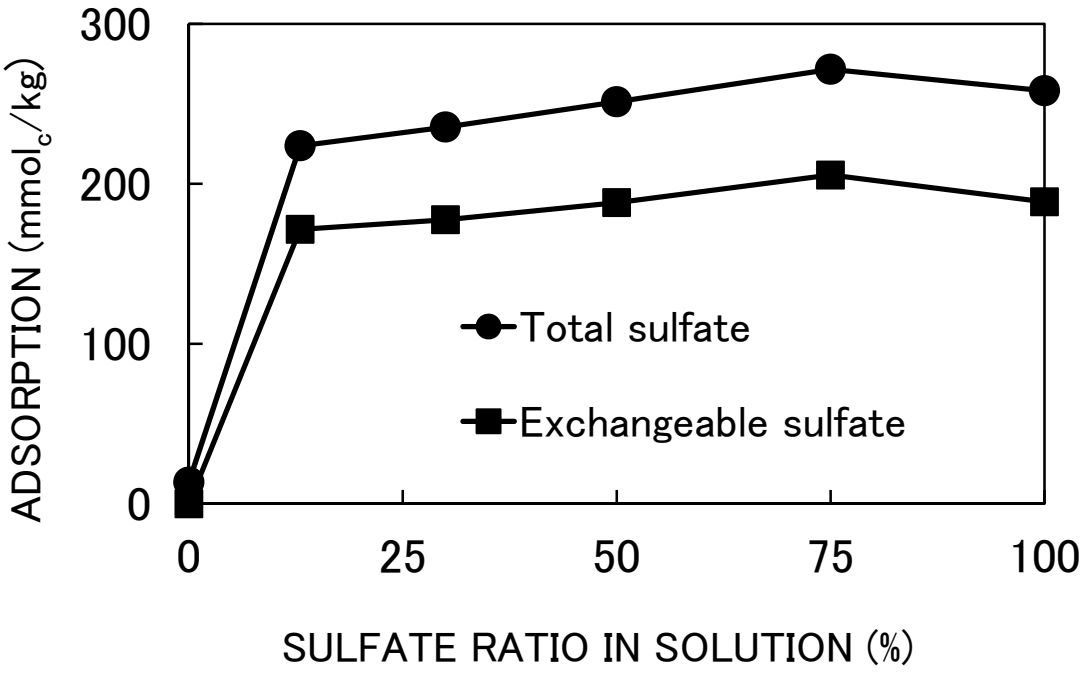

Fig. 2. SO_4 adsorption on the allophanic Andisol at pH 4.3 and 0.1 $mol_c\ m^{-3}$.

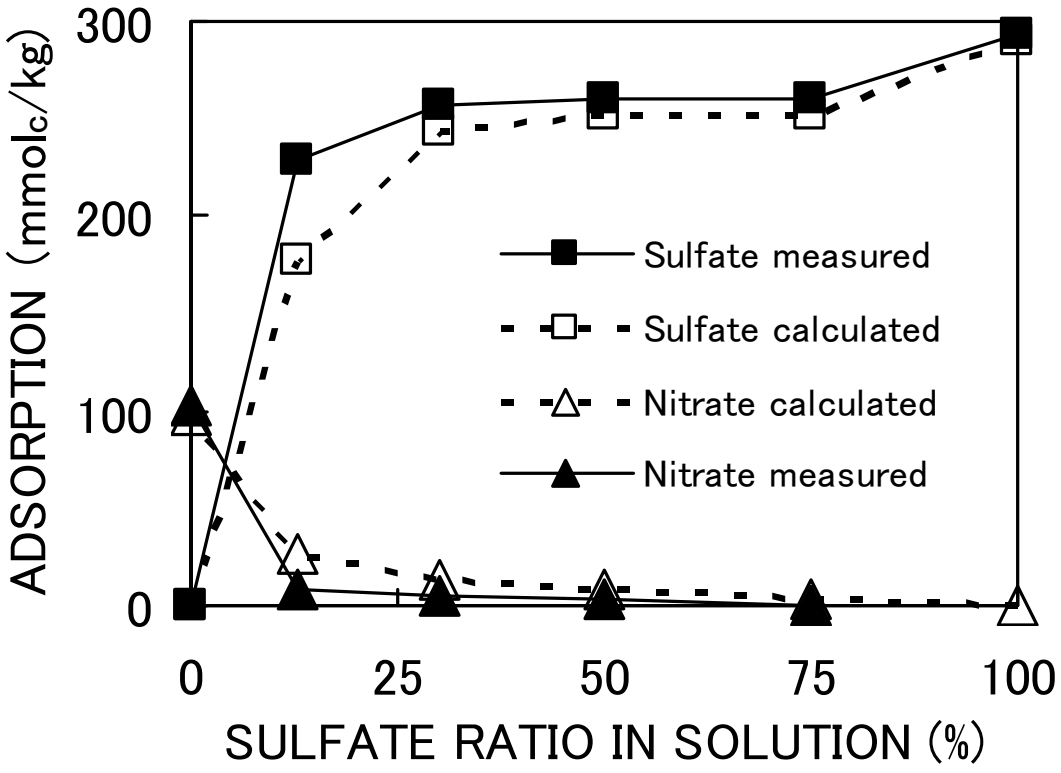

Fig. 3. The Gouy-Chapman model estimations of NO_3 and SO_4 adsorption compared to the experimental data at pH 3.3.

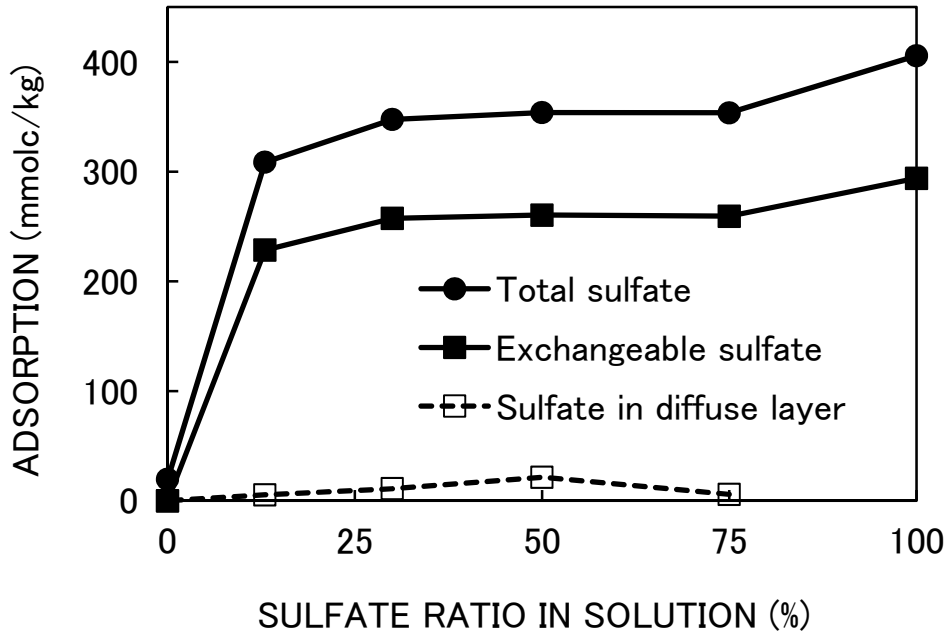

Fig. 4 SO_4 adsorption at pH 3.3. SO_4 in the diffuse layer was calculated by the Stern-Gouy-Chapman model.

Table 1. Physical and chemical characteristics of the soil.

(National Institute of Agricultural Sciences, 1984[28])

Soil characteristics	
Coarse sand	1.7 %
Fine sand	11.2 %
Silt	37.5 %
Clay	49.5 %
Amorphous material (with allophane + imogolite)	41.4 %
Organic C	1.16 %
Texture class	Heavy clay
Porosity	82.4 %
Bulk density	510 kg m^{-3}
Cation exchange capacity	
pH 5	5.7 $cmol_c$ kg^{-1}
pH 7	10.6 $cmol_c$ kg^{-1}
Anion exchange capacity	
pH 5	10.3 $cmol_c$ kg^{-1}
pH 7	0.6 $cmol_c$ kg^{-1}